NAVAL POSTGRADUATE SCHOOL
Monterey, California

THESIS

EXPERIMENTAL STUDIES OF TWO-WAY SINGLE ELEMENT TIME REVERSAL IN A NOISY WAVEGUIDE

by

John P. Stokely

June 2001

Thesis Advisor: Andrés Larraza

Thesis Advisor: Mitchell N Shipley

20010816 005

REPORT DOCUMENTATION PAGE		*Form Approved OMB No. 0704-0188*

1. AGENCY USE ONLY *(Leave blank)*	2. REPORT DATE June 2001	3. REPORT TYPE AND DATES COVERED Master's Thesis

4. TITLE AND SUBTITLE: Title (Mix case letters) Experimental Studies of Two-Way Single Element Time Reversal in a Noisy Waveguide	5. FUNDING NUMBERS
6. AUTHOR(S) Stokely, John P.	
7. PERFORMING ORGANIZATION NAME(S) AND ADDRESS(ES) Naval Postgraduate School Monterey, CA 93943-5000	8. PERFORMING ORGANIZATION REPORT NUMBER
9. SPONSORING / MONITORING AGENCY NAME(S) AND ADDRESS(ES) N/A	10. SPONSORING / MONITORING AGENCY REPORT NUMBER

11. SUPPLEMENTARY NOTES The views expressed in this thesis are those of the author and do not reflect the official policy or position of the Department of Defense or the U.S. Government.

12a. DISTRIBUTION / AVAILABILITY STATEMENT Approved for public release; distribution in unlimited	12b. DISTRIBUTION CODE

13. ABSTRACT *(maximum 200 words)*

As the United States Navy considers operation closer to shore, it must account for the impact of shallow water ocean environments on the performance of active sonar. Multi-path propagation and high ambient noise in these areas pose a unique detection challenge for current sonar systems. A possible solution for this problem involves the use of processing that is actually enhanced by multi-path propagation, and can perform in the presence of in-band noise. Time-Reverse Acoustics (TRA) has been used with many transducer elements to focus acoustic energy in a very small region. Used as a single element active sonar, it can focus the return of an active pulse at the receiver location.

To test the performance of a TRA-based sonar in the presence of noise, ultrasonic signals were used in a laboratory waveguide, so that the scale of wavelength to water depth approximates a shallow channel with a flat, lossy bottom. Several sequences of a traditional sinusoidal pulse and the time-reversed reception were performed with varying noise levels. The gain in detection signal-to-noise ratio (SNR) was on average $+7.3\pm0.8$dB using TRA. Further, the TRA processing provided a noticeable detection when noise had completely obscured the reception of the initial pulse.

14. SUBJECT TERMS Time Reverse Acoustics, Active Sonar, Signal-to-Noise Ratio (SNR), Waveguide			15. NUMBER OF PAGES 70
			16. PRICE CODE

17. SECURITY CLASSIFICATION OF REPORT Unclassified	18. SECURITY CLASSIFICATION OF THIS PAGE Unclassified	19. SECURITY CLASSIFICATION OF ABSTRACT Unclassified	20. LIMITATION OF ABSTRACT UL

THIS PAGE INTENTIONALLY LEFT BLANK

EXPERIMENTAL STUDIES OF TWO-WAY SINGLE ELEMENT TIME REVERSAL IN A NOISY WAVEGUIDE

John P. Stokely
Lieutenant Commander, United States Navy
B.S., University of Connecticut, 1988

Submitted in partial fulfillment of the
requirements for the degree of

MASTER OF SCIENCE IN APPLIED PHYSICS

from the

## NAVAL POSTGRADUATE SCHOOL
June 2001
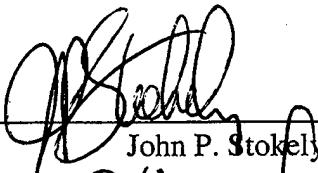
Author: _____
John P. Stokely

Approved by: _____
Andrés Larraza, Thesis Advisor
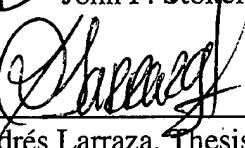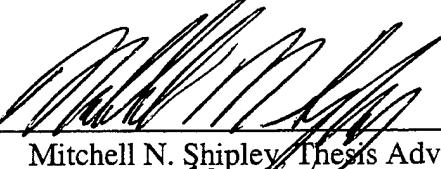
_____
Mitchell N. Shipley, Thesis Advisor
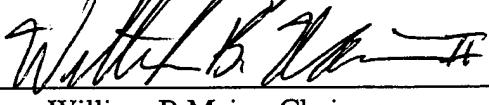
_____
William B Maier, Chairman
Department of Physics

THIS PAGE INTENTIONALLY LEFT BLANK

ABSTRACT

As the United States Navy considers operation closer to shore, it must account for the impact of shallow water ocean environments on the performance of active sonar. Multi-path propagation and high ambient noise in these areas pose a unique detection challenge for current sonar systems. A possible solution for this problem involves the use of processing that is actually enhanced by multi-path propagation, and can perform in the presence of in-band noise. Time-Reverse Acoustics (TRA) has been used with many transducer elements to focus acoustic energy in a very small region. Used as a single element active sonar, it can focus the return of an active pulse at the receiver location.

To test the performance of a TRA-based sonar in the presence of noise, ultrasonic signals were used in a laboratory waveguide, so that the scale of wavelength to water depth approximates a shallow channel with a flat, lossy bottom. Several sequences of a traditional sinusoidal pulse and the time-reversed reception were performed with varying noise levels. The gain in detection signal-to-noise ratio (SNR) was on average +11.7dB using TRA. Further, the TRA processing provided a noticeable detection when noise had completely obscured the reception of the initial pulse.

THIS PAGE INTENTIONALLY LEFT BLANK

TABLE OF CONTENTS

THIS PAGE INTENTIONALLY LEFT BLANK

LIST OF FIGURES

THIS PAGE INTENTIONALLY LEFT BLANK

ACKNOWLEDGMENTS

THIS PAGE INTENTIONALLY LEFT BLANK

I. INTRODUCTION

In the past ten years, a large body of work has been generated pertaining to time-reverse acoustics (TRA), and the surprising quality of temporal and spatial focusing of acoustic energy. At its heart, the process relies on reciprocity. If a wave front is finely sampled in both time and space, that wave pattern may be generated in reverse by transmitting the time-reversed signal detected at each location. As the reverse wave pattern propagates, it focuses briefly on the original source location.

As an example, consider lining the shore of a small pond with reversible transducers. It should be possible to transmit from these transducers in such a way as to get the surface ripples to momentarily focus at the exact location a rock was dropped. The necessary transmit signal from each of the shoreline elements turns out to be nothing more complicated than the reverse of the incoming wave pattern.

Many applications have been envisioned which rely on TRA to focus acoustic energy. Mathias Fink (1999) proposed using the method for lithotripsy, a medical procedure to destroy kidney stones. Fink (1998) has also proposed using TRA for non-destructive testing of construction materials. At the Naval Postgraduate School, investigation of the technique's applicability to underwater communications has shown not only an ability to focus the acoustic signal, but exploit a natural encryption afforded by the environment (Heinemann, 2000). All of these applications share the common trait of tightening the focus of the time-reversed pulse, in order to maximize the amount of energy on a minimized region called the 'retrofocus.'

1

The most salient feature of these experiments is the use of a time reverse mirror (TRM) consisting of a number of transducers operating at high sample rates. If an incoming wavefront is more finely sampled spatially and temporally, the generated reverse wave pattern will be more faithful and the retrofocus will more closely resemble the original source. For much of their work, Roux and Fink (2000) use a TRM consisting of up to 96 transducers spaced at approximately half-wavelength intervals. They have predicted and experimentally demonstrated significant spatial focusing and temporal compression of acoustic energy. Temporal compression means that the time-reversed signal at the retrofocus is similar in temporal extent to the initially transmitted signal. Spatial focusing refers to the size and location of the retrofocus as compared to the original source.

These studies began with an ocean experiment conducted by Parvelescu, et al, (1965, republished 1995) in which the temporal compression of a reversed signal was demonstrated using a single transmit and single receive element, separated in range. Single-element time reversal will not produce a retrofocus in a free-space environment. Instead, multi-path propagation must be present so that the temporal record alone can be used to reproduce wavefront curvature. Shallow water ocean environments, or more locally a laboratory waveguide provide sufficient multi-path information to make the effect possible.

In this thesis a single element TRM is used to investigate applications to sonar technologies. This specific application of time reversal uses the notion that although a single-element TRM will not produce optimal focus, there is a distinct detection advantage to be gained over a conventionally transmitted pulse. Used as an active sonar

2

system, TRA could enhance detection of submerged objects. In this case, a loose focal region significantly larger than the source may actually be desired, due to the relative motion between target and the detection platform.

Time reversal applied to active sonar affords the specific advantage of providing a robust and reliable detection in shallow water environments where multi-path propagation and reverberations make interpretation of current sonar information challenging. TRA is less time-consuming. There are no computer models to run that will select optimal pulse parameters. Nor are there environmental sampling requirements, beyond the local speed of sound. All knowledge of the propagation is implicitly carried in the reception of a test pulse. One might also argue that a sonar system based on a single-element TRM is within reach of being operationally fielded. No special configuration of transducers is required. The system could be implemented with software changes to existing sonars. With these ideas in mind, this thesis might be considered a feasibility study for applying TRA to an actual sonar system, initially using a more demanding single-element approach. An outstanding question for such a system is performance in the presence of in-band noise.

Numerical studies have shown that the TRA process will still provide an enhanced detection in the presence of gaussian noise (Khosla and Dowling 2001). Under these conditions, the TRA retrofocus size lacked any trend with increasing noise level and was instead primarily governed by the acoustic frequency and the characteristics of the propagation path.

Ambient noise creates at least two challenges for the TRA process. First, the array always rebroadcasts some or all of the noise it receives, and thus introduces additional

noise to the environment, which can obscure the retrofocus. Second, the ambient noise may overwhelm an otherwise acceptable retrofocus field. Additionally, the maximum possible signal amplification is lower in noisy environments because the array wastes power re-broadcasting non-signal.

In this work, a single-element sonar system using TRA processing is operated in an ultrasonic waveguide in the presence of a varied noise field levels. The first two effects listed in the above paragraph are experimentally verified. The signals transmitted, however, were not of a large enough amplitude to test the limits of the array, as described in the third effect. Ultimately, conclusions are drawn as to the effectiveness of the TRA system in the presence of the noise field.

The organization of this thesis is as follows: Chapter II outlines the theory behind TRA and its extension to single-element transmission/reception in a waveguide. Chapter III describes the experimental setup and the conduct of the testing done to evaluate the performance of TRA in the presence of in-band noise. Chapter IV contains a sample of the collected data, and an analysis of the results. Chapter V draws some conclusions from this work and contains recommendations for follow on research.

II.   TIME REVERSED ACOUSTICS THEORY

It has been stated that in free space, the creation of a set of waves that will precisely retrace the complex paths of an incoming wavefront requires an array of transducers operating at a high sample rate. The work of this thesis however, involves producing that effect with a single element only.

To resolve this apparent difficulty, this chapter begins by outlining the behavior of a signal within a laboratory waveguide. The method of images is then employed to produce an array of virtual sources, with a number of elements equal to the number of propagating modes in the waveguide. Once the connection is made between the waveguide and free-space, it is possible to apply time-reversal techniques to the free space representation of the sound field and expect the results to carry over to the waveguide.

A.   PROPAGATION IN A WAVEGUIDE

The wave equation for simple harmonic waves propagating in an acoustic duct satisfies the homogeneous Helmholtz equation

$$\left[\nabla^2 + \left(\frac{\omega}{c}\right)^2\right] p = 0 \qquad (2.1)$$

where p is the pressure, c is the thermodynamic speed of sound in the medium, and ω is the angular frequency of the wave. The tank used for these experiments has anechoic tiling on the vertical surfaces to reduce sidewall reflection. If this reduction is assumed to be perfect, variations in the transverse direction can be ignored. It is therefore

appropriate to seek solutions to the Helmholtz equation in cylindrical coordinates, allowing for spreading from the source. Setting the r-axis parallel to the axis of the waveguide, the time-independent behavior of the pressure in Equation (2.1) satisfies

$$\left[\nabla^2 + k^2(r)\right]\psi(r,\omega) = 0 \qquad (2.2)$$

Equation (2.2) introduces the wavenumber $k = \omega/c$, a function of sound speed and angular frequency. Because the propagation is in two dimensions, the wavenumber is considered to have vertical and horizontal components, k_z and k_r. They are related by:

$$k^2 = k_z^2 + k_r^2 \qquad (2.3)$$

It is instructive to consider the tank as a Pekeris waveguide. (Jensen, et al 2000) Instead of regarding the bottom to be rigid and lossless (an ideal waveguide), in the Pekeris waveguide it is more realistically modeled as an infinite fluid halfspace, having density and sound speed to match those of the floor. This allows energy to be transmitted across the water-bottom interface, introducing a loss mechanism to the waveguide propagation. Figure 2.1 is a schematic of such a waveguide.
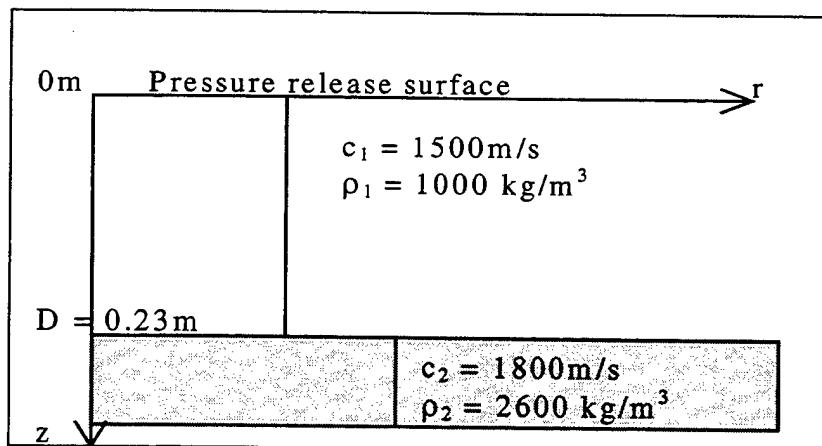
Figure 2.1   Pekeris waveguide with pressure-release surface and penetrable fluid bottom. The bottom parameters correspond to concrete. After Jensen, et al (2000).

In developing normal mode solutions to the Helmholtz equation, continuity of particle displacement and of bottom pressure must be considered. This leads to the following characteristic equation for vertical wavenumbers of the normal modes in the two fluid spaces, designated $k_{z,1}$ and $k_{z,2}$ respectively:

$$\tan(k_{z,1}D) = -\frac{i\rho_2 k_{z,1}}{\rho_1 k_{z,2}} \tag{2.4}$$

In order for a mode to propagate without loss (other than geometrical spreading) the horizontal wavenumber must be real. It can be shown that Equations (2.3) and (2.4) yield real solutions for k_r only in the interval

$$|k_2| < |k_r| < |k_1| \tag{2.5}$$

Therefore, no modes exist with real propagation wavenumbers less than $k_2 = \omega/c_2$. The simple explanation of this is that for wavenumbers smaller than this, the grazing angle of the plane wave would be above the critical angle for the interface, causing significant amounts of energy to leak out of the duct and into the bottom.

If a source is placed at a depth z_s it will excite a number of modes in the waveguide and propagate accordingly. The wavefront produced can be viewed as a superposition of normal modes excited by the source. The approximate modal solution for the Pekeris waveguide takes the following form:

$$\psi(r,z) \approx -\frac{iS_\omega}{2D}\sum_{m=1}^{M} a_m k_{rm} \sin(k_{zm}z)\sin(k_{zm}z_s)H_0^{(1)}(k_{rm}r) \tag{2.6}$$

with S_ω the frequency dependent source strength and $H_0^{(1)}$ the Hankel function of the first kind. The modal excitation $(a_m k_{rm})$ is a function of the applied frequency (Jensen, et al 2000).

The modal expansion in Equation (2.6) is truncated to M modes with real propagation wavenumbers. M will increase with the frequency of the source. When source frequency is lowered, the propagation wavenumber of a particular mode decreases according to the characteristic (2.4). A mode is said to be cut off when the modal wavenumber reaches the limit $k_{rm} = k_2$. The radial cutoff frequency for mode m is determined from the characteristic equation by inserting $k_{rm} = k_2 = \omega_{0m}/c_2$ to yield the following expression (Jensen, et al, 2000):

$$f_{0m} = \frac{\omega_{0m}}{2\pi} = \frac{(m-0.5)c_1 c_2}{2D\sqrt{c_2^2 - c_1^2}} \qquad \text{for } m = 1,2,3\ldots \qquad (2.7)$$

The signal carried by mode m will propagate with the horizontal speed u_m, the group velocity, given by

$$u_m = \frac{dr}{dt} = \frac{d\omega}{dk_{rm}} \qquad (2.8)$$

At cutoff, the group velocity equals the bottom sound speed. It quickly drops to below the sound speed in the fluid layer then rises, asymptotically approaching c_1 at high frequencies. Thus, signal information in higher propagating modes will arrive after the lower modes (Jensen, et al, 2000).

The end result of this discussion is that a single receiver in a waveguide at some distance from the source will record the arrival of different modal components of a signal

at different times. If the dimensions of the waveguide are known and for an arbitrarily high sample rate, the time record alone will provide enough information to extract the geometric information contained in the signal.

Figure 2.2 shows a typical reception following the transmission of a short sinusoidal pulse. Significant lengthening of the signal due to the coherent addition of late-arriving modes is clearly seen. Also evident are the differing amplitudes with which these modes arrive. The amplitude difference comes from a differing number of interactions with surface or bottom (neither of which are perfectly reflecting in practice).

Transmitted
Signal
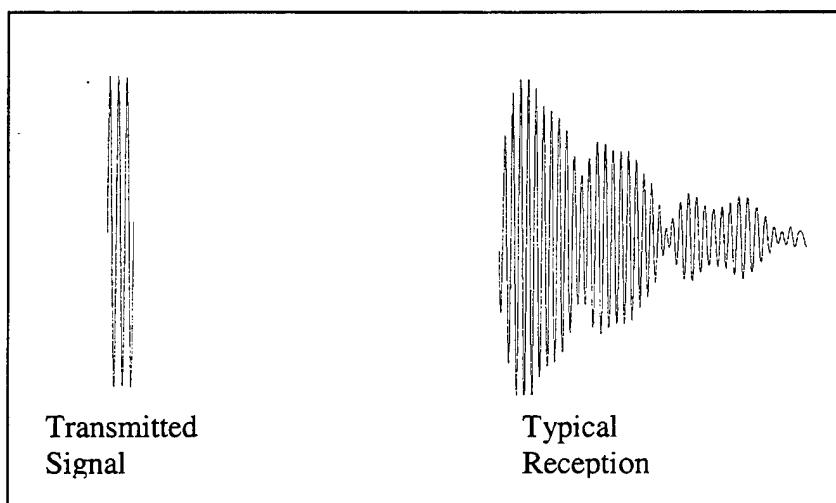
Typical
Reception

Figure 2.2   A typical reception is shown for the transmitted signal on the left. The time scale for both signals is the same.

B. METHOD OF IMAGES

The method of images provides a convenient way to consider the modal structure of waveguide propagation as analogous to a free-space phenomenon (Kinsler, et al, 1982). Here, the geometric paths of the propagating modes are viewed as emanating from several "virtual sources" spaced at intervals of the waveguide depth, as shown in Figure 2.3.

Z_0-2D

θ

0

Z_0

Z_0+D

Source and Images

Receiver
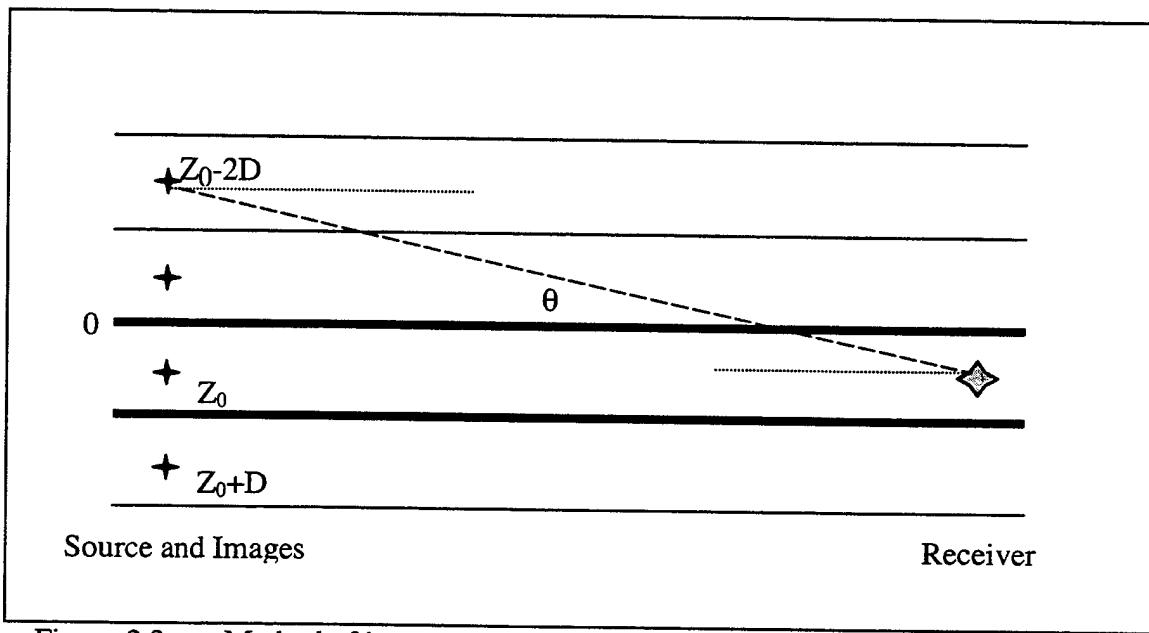
Figure 2.3   Method of images applied to a waveguide source to produce an array of virtual sources.

The theoretical number of image sources is infinite. The higher order modes, however, will have reduced weighting due to imperfect reflections when interacting with the bottom or surface. In the ultrasonic waveguide, where dimensions of the transducer are not small compared to a wavelength, this number will be further limited by the angular directivity of the elements both in transmission and reception.

The imperfect reflections mentioned above produce attenuation as a function of range that to a first approximation is represented by:

$$R(\theta) = R_1^n(\theta)(-1)^m \qquad (2.9)$$

Here, $R_1(\theta)$ is the reflection coefficient measured at the water-bottom interface at a grazing angle θ, and n refers to the number of bottom interactions for the mode with propagation angle θ. Similarly, m is the number of surface interactions for this mode, each resulting in a $180°$ phase shift. For a given propagation angle, a larger range will produce more attenuation. The coefficient R_1 becomes complex for propagation above the critical grazing angle for the bottom interface. This means that long-distance propagation in a waveguide will be limited to a cone whose half-angle is equal to the critical angle (Roux & Fink, 2000).

The experiments conducted in this work use ultrasonic signals emitted and received by cylindrical transducer elements with dimensions on the order of a wavelength (a more complete description of the equipment set-up is contained in Chapter III). This leads to an angular directivity, $ang(\theta)$, which affects the acoustic field both in transmission and reception. For a launch angle θ, this directivity is approximated in the far-field by an attenuation coefficient:

$$ang(\theta) \propto \frac{\sin(\tfrac{1}{2}ka\sin(\theta))}{\tfrac{1}{2}ka\sin(\theta)} \qquad (2.10)$$

where, k is the wavenumber at the center frequency, and a is the size of the transducer. Angular directivity will limit the long-range propagation to a cone whose half-angle is determined by transducer characteristics (Roux & Fink, 2000).

For the tank dimensions and transducer characteristics of this experiment, the limitation imposed by the critical angle is the dominant effect.

The above considerations can be used to quantify the number of trapped modes that propagate a specific distance in the waveguide. The method of images then effectively exchanges these M total modes for a virtual array of $2M$ equally spaced and identical sources (See Figure 2.2).

In the system under test in these experiments the source and receiver are co-located. Two-way propagation off a scatter source must be considered. The scatter source (target) acts like a point-source for the reflected field. This reflected signal is not a pure sinusoidal signal like the initial transmission. Rather, it is a superposition of the modes trapped in waveguide propagation that were excited by the original signal. The reflected signal returns to the receiver down a similar path as the arrival, so each component of the reflected signal excites those same M modes on the return trip. Thus, the final received signal will consist of $2M$ sources each transmitting M individual signals. The final received signal will contain $2M^2$ total echoes, many of which will overlap and coherently interfere. The characteristics of the interference pattern will be dependent on range as well as target and source depths.

C. TIME REVERSAL APPLIED TO A FREE SPACE ARRAY

In the free-space visualization, each image of the source and each image of the receiver is weighted according to the attenuation coefficients of Equations (2.9) and (2.10). Thus, the further the images are from the waveguide (i.e., higher order modes) the smaller their overall contribution to the acoustic field (Roux & Fink, 2000).

12

A time-reversal experiment consists first of transmitting a pulse (by all of the image sources) and then time-reversing the acoustic field back (from all the image receivers). For a source at coordinates $r_0=(0,z_0)$, the N total image sources will be located at $r_s = (0,z_0\pm sD)$, for integer s. For a single-element time reverse mirror (TRM), a distance L from the source, the N total TRM images are located at $r_p = (L,z_0\pm pD)$ for integer p.

To compute the field after time reversal, the Green's functions between the sources at time 0 and the TRMs at time t are first computed. Similarly, the Green's functions between the TRM and the sources must also be calculated, to account for backward propagation. Included in this, are the attenuation coefficients of Equations (2.9) and (2.10) to account for weighting.

The time-reverse field at point r is then found with the formula:

$$P_{TR}(r,t) = \sum_{s}\sum_{p}\left[G\left(r,t\,|_{r_p,0}\right)\otimes G\left(r_p,T-t\,|_{r_s,0}\right)\right]\otimes f(T-t) \qquad (2.11)$$

Where f(t) is the transmitted signal and the time T is such that G=0 for t>T. The symbol $\otimes$ denotes convolution. (Roux & Fink, 2000).

The expression in square brackets in Equation (2.11) can be used to show that the time reversal process produces focusing. By examining the time-reversed field at the point of retrofocus, that is, at $r = r_p$ in Equation (2.11), and remembering that there is no sound speed gradient, this portion of the equation can be seen as a Green's function correlated with itself, which is a form of a matched filtering operation. The sum over all elements forms a spatial matched filter, hence the field is focused in space. (Kuperman, et al, 1998)

13

In the case of the uniform sound speed associated with the Pekeris waveguide, the acoustic propagation between the sources and the receivers is described by the 3D free-space Green's function, which leads to the following simple approximation:

$$G(r_p, t \mid_{r_s, 0}) \approx R(\theta) ang^2(\theta) \frac{\delta(t - |r_p - r_s|/c)}{|r_p - r_s|}$$

(2.12)

with

$$\theta = \cos^{-1}\left(\frac{|r_p - r_s|}{L}\right).$$

(2.13)

Note that the angular directivity is squared because the sound is transmitted and received by identical transducers (Roux & Fink, 2000).

The array gain for a vertical array of sources is expected to be $10\log(N)$, for N transducers. This value could be as high as $20\log(N)$, depending on the relative source strength of the array elements. (Khosla and Dowling, 2001). For this experiment, the single element transmit/receive scheme can be approximated by a virtual array of sources not equally weighted. The observed array gain should therefore be toward the low end of the range above.

III. EXPERIMENT DESCRIPTION

This chapter begins with a brief description of the tank and the apparatus used to conduct the experiment, and describes the experiment used to evaluate time-reversed sonar in a noisy environment.

A. APPARATUS

1. Tank Description

The experiment is conducted in a fiberglass coated wooden tank. The sidewalls are covered with anechoic tiles to reduce the side-reflections and remove cross-range interference. The inner dimensions are roughly 15.3 meters long by 1.2 meters wide, with anechoic tiles vertically along the sidewalls to a height of 28 cm. The tank is filled with fresh water to a level of 23.5 cm, a level below the top of the anechoic. The tiling reduces echo reflection by about 25 dB across the frequency range 20-100kHz.

The tank approximates a horizontally infinite waveguide with a nearly rigid bottom and pressure release surface, and is shown in Figure 3.1
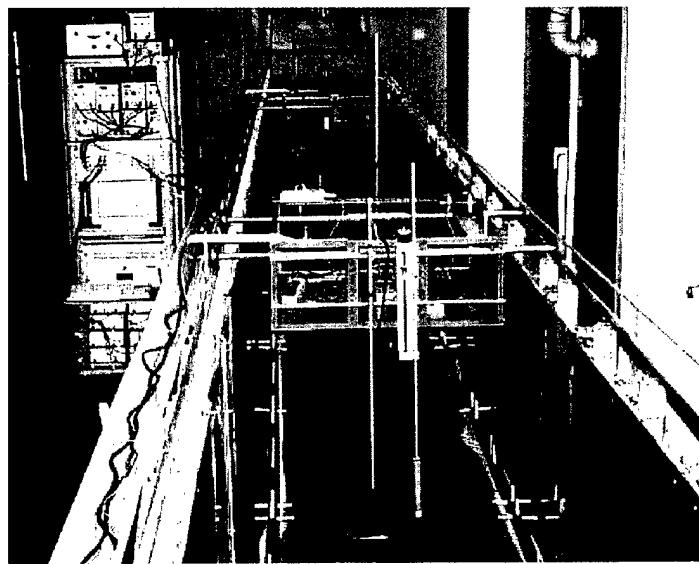
Figure 3.1   Test Tank with PC operating console.

2. Transducer Array

The source and receive elements are co-located within one array. Made by EDO

Electric-Ceramic Products, it consists of ten cylindrical piezoceramic elements vertically

aligned in a PVC tube, 3.8 cm in diameter and 30.5 cm in length. The experiment was

conducted transmitting on element #4 and receiving on element #7 (shown in Figure 3.2)

for a rough source depth of 10cm and a receiver depth of 16 cm
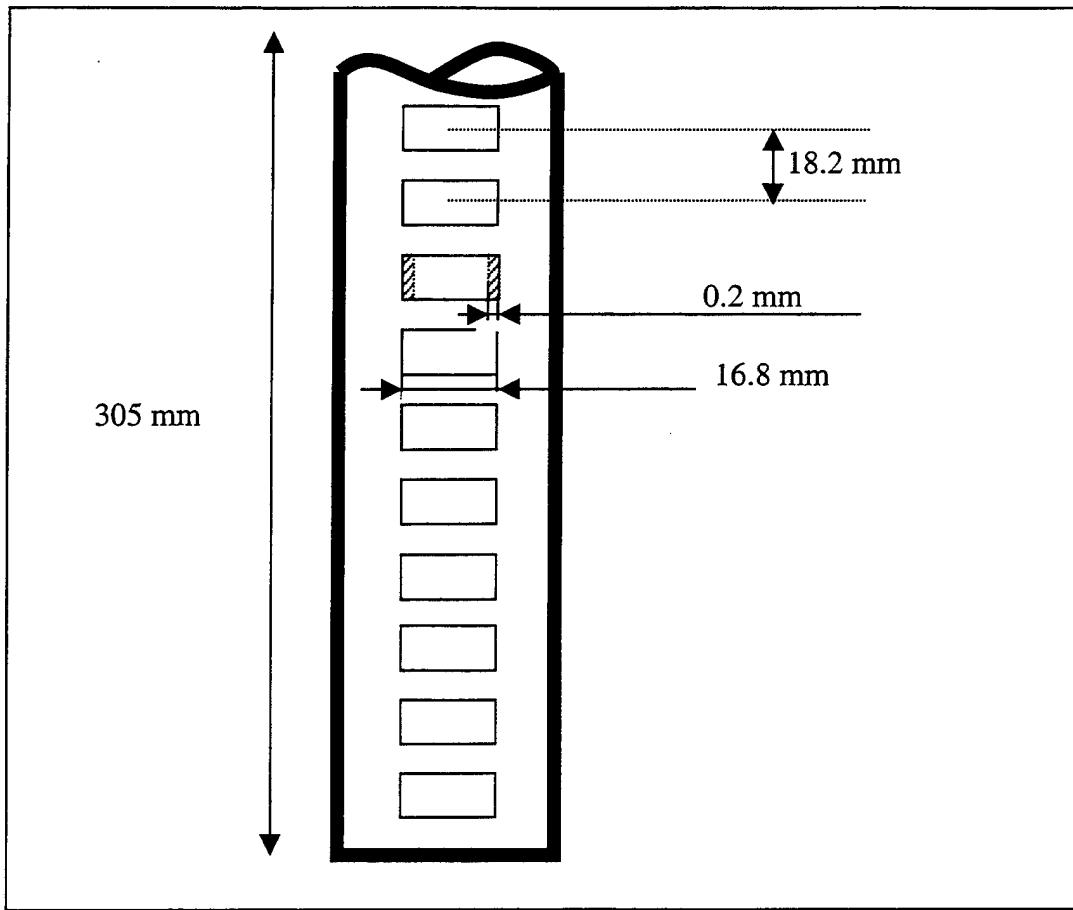
Figure 3.2   Ten-element transducer arrays made by EDO Electro-Ceramic Products. After Heinemann (2000).

3. Computer and Operating System

All operations of the Time Reverse Acoustic Pulse (TRAP) Sonar System are closely linked to the central operating computer, with a 266MHz Pentium II processor running Windows 98 software.

Signals are generated with CompuGen 1100 function generator cards, and data capture is done with CompuScope 512 oscilloscope cards. These cards are addressed via separate software files, and called with MATLAB programs.

The MATLAB software controls all aspects of the sonar system operation, including definition of the signals, editing captured data (including cutting and time-

reversing and re-transmitting), visualization and storage of the data. Most functions are controlled with a single graphical user interface.

4. Functional Description of TRAP Sonar System

The system used in this experiment employs single transmit and receive elements that are roughly co-located within the isospeed waveguide. This section describes the sequence of events that occurs to produce a time-reversed reception:

First, there is the transmission of the initial signal (IS). It is a 3 cycle sinusoidal pulse at 73 kHz with $\pm$ 25V peak amplitude, transmitted from a small cylindrical element. This signal then propagates down the waveguide, with some energy reflected back toward the source by a target. The initial signal is displayed as a voltage vs pulse width. The sinusoidal pulse described above has a 6.1cm pulse width.

At the instant of transmission, return data, referred to as the first reception (FR), begins to queue from the receive element, approximately co-located with the source. The TRAP program samples this data at a maximum rate of 5MHz for approximately 300ms. This corresponds to a two-way travel distance of roughly 22m, using 1500m/s as an approximate speed of sound. The maximum detection range can be extended by lowering the sample rate, but because 22m is significantly longer than the tank in which the experiment was conducted, the sample rate was left at its maximum value. An operator-selected portion of the FR data is displayed in terms of received voltage vs. range.

A subset of the FR containing the potential target return is cut and digitally flipped left to right. It is then amplified, so that the peak of this time-reversed (TR) signal is $\pm$25V, similar to the initial signal. Similar to the IS, this is displayed as voltage vs. pulse width. Because transmission to reception involves two-way propagation, a

18

range window captured from the FR data will correspond to a pulse length that is twice the extent of the first reception captured range.

Upon transmission of the TR signal, return data begins queuing as the second reception (SR). As before, the sampling rate is selectable, with a maximum rate at 5MHz, and the data is displayed as received voltage vs. range from the source. The operator selects the horizontal scale of the FR and SR windows. The vertical scales of the two reception graphs are the same and chosen automatically such that the peak value of the SR is displayed within the confines of the GUI window.

The received data is digitally filtered from 55-85kHz to reject ambient noise within the test facility.

5. Noise Generation

Noise was introduced into the tank by through an ITC model 395 projector, generated by a General Radio 1390 Random Noise Generator. The noise generator was set to produce a varying level of white noise across a frequency band of 0-500kHz. The noise was filtered by a Krohn-Hite 3988 Dual Channel Filter set for 55-85kHz Bessel-type filtering with unity gain. It is important to note that the bandwidth of the noise was set to closely approximate the bandwidth of the transmitted signal.

6. Scaling the Tank to a Real Ocean Waveguide

The sound speed of water in the tank is measured to be about 1504 m/s. The corresponding wavelength for a 73kHz sinusoid is 2.06 cm. Thus the height of the water-column is 11.3 wavelengths of the applied signal. If the applied signal were 250Hz, the wavelength would be 6.02 m, corresponding to a water depth of 68m. The length of the

tank would scale to 3.5km. If the signal were 500Hz, the wavelength is 301cm, corresponding to a water depth of 34m, and a range of 1.8km.

In other words, the tank can be thought to approximate a shallow straight of water, of indefinite horizontal extent. With a traditional active sonar system, this environment would present an enormous challenge. While it is true that the laboratory waveguide idealizes the bottom features and contains no volumetric scatter sources that would otherwise plague a sonar system operating in the shallows, the results obtained here can be directly extended to an actual ocean channel.

B. TEST CONDITIONS

1. Equipment Lineup

With a set of standard target geometry and tank conditions, several TRAP sequences were taken at varying noise levels. The only variable throughout the experiment was the output of the noise generator.

Standardized test conditions are shown in Table 3.1.

Tank	Water Depth: 23.5 cm Water Temp: 18° C.

Target	Aluminum Submarine target, Approx 15 cm long, port 90° aspect
	Location:
	        Range 7.40 m from the source. (10.4 m from front of tank)
	        Keel Depth: 13 cm
	        54 cm from edge of tank (approximately centered)

Source	Single Element (Array element #4) Depth ~10cm
	Source Location:
	        3.04 m from front wall of tank
	        56 cm from near edge (approximately centered)
	Transmit signal: 3 cycles, 8Vpk @ 73kHz.
	Amplifier: x5

Receiver	Single Element (Array Element #7) Depth ~ 16cm
	Source Location:
	        3.04 m from front wall of tank
	        56 cm from near edge (approximately centered)
	Pre-amp Settings:
	        Gain: 2 x 10^3,
	        Filter: 1kHz to 300 kHz, with 6dB/decade roll-off

Table 3.1   Standard Equipment Lineup and Target Geometry

2.   Data Saving and File Naming Conventions

The complete representation of a TRAP sequence involves the four time records described in a previous section. They are labeled as T-xxx-QQ.ext. Where 'T' is for "trial" (system default) and xxx is the numeric number of the sequence, usually beginning with 100. 'QQ' takes values of IS, FR, TR, or SR, as appropriate. The extension 'ext' is an operator selectable descriptive string used to distinguish a particular set of runs. Writing "Txxx.ext" simultaneously refers to all four files.

The convention used for naming the sequence files for this experiment is TxxxNyy. Where xxx is a three-digit number ranging from 100 to 150 and yy is a two-

digit number from 00 to 13, representing the number of step increments from the noise generator.

C.   DATA ACQUISITION

With the noise generator off, a single TRAP sequence was performed to verify the operation settings and save path. Then 50 more identical sequences were performed in automated succession. This initial data set represents the highest SNR condition possible, and is saved as N_00.

Gradually increasing the output level of the noise generator, the process was repeated to obtain similar sets of TRAP sequences. A total of 13 different noise levels were examined, with 51 TRAP sequences taken at each increment.

The presentation of the data and the resultant analysis form the basis for the next chapter.

IV. DATA ANALYSIS AND RESULTS

This chapter begins with a description of the method used to calculate the signal to noise ratio (SNR) of the first and second reception returns. A representative sample of the raw data taken and a qualitative discussion of the performance of the TRA process with increasing noise follows. Finally, a comparison of the data between noise levels is made. From this comparison it is seen that the time-reversal process produces a reliably enhanced return even when the first reception is completely masked by noise.

A. CALCULATION OF SNR

The data received in a TRAP return is a time record of voltage information. It was therefore simplest to consider signal level and noise level in terms of voltage received. It is further desired that the SNR for an individual TRAP sequence is calculated solely from information contained in that sequence.

The target geometry is known, and fixed, so that each reception record may be divided into a target window, and a non-target window. The actual target location was 7.40m from the source, so for the first reception records, the target window was set at 7.0-8.0m. This window will contain both signal and noise. The maximum received level in this window will be considered signal + noise, $(S+N_s)$.

The remainder of the information, i.e., all data contained in the non-target window contains only noise. The noise is considered zero-mean gaussian, and so can be characterized completely by the variance, σ_n^2 (Khosla and Dowling, 2001). The noise level chosen then is the variance of the data outside the target window.

23

From the preceding information, signal-to-noise ratio can be found by first obtaining the signal level, S, as

$$S = (S + N_s) - N \tag{4.1}$$

where N is the maximum level received in the non-target window. If it is assumed that $(N_s - N)$ will be negligible, i.e., that the peak level of noise is not significantly different inside or outside the target window, then the desired SNR can be calculated as follows:

$$SNR = 10\log_{10}\left(\frac{((S + N_s) - N)^2}{\sigma_n^2}\right) \tag{4.2}$$

This scheme can be applied to either the first or the second reception. Worth noting is that a negative SNR, while numerically possible has little meaning for this sonar system. This is because the data driven SNR measurement scheme cannot evaluate a signal that is less than the noise in the signal window. The values displayed have a positive value or they are considered zero.

B.   ANALYSIS OF INDIVIDUAL DATA SETS

This section presents three examples of raw data for TRAP sequences at varying noise levels. It is instructive to examine the salient characteristics of each one, and compare the behavioral trends with increasing noise.

1.   Low Noise

Figure 4.1 is a TRAP Sonar display. The figure in the upper left is the initial signal, 3 sinusoidal cycles at 73kHz. The horizontal scale is pulse width in meters. The lower left window shows the resultant first reception (FR). For all TRAP sequences analyzed here,

24

the TR window was set from 7.0 to 8.0 meters in range on the first reception. The upper right window of Figure 4.1 shows the TR signal. Notice that the vertical scale on the two upper windows is the same. The horizontal scale of the TR signal plot is set automatically. It is also scaled as pulse width in meters. Finally, the lower right graph shows the second reception (SR) data, received upon transmission of the TR signal. The vertical scale on the two lower plots is the same. Set automatically by the max level received in the SR window. This is for ease of visual comparison.

The TRAP sequence shown in Figure 4.1 is an example of low-noise data. It was taken as part of the N_00 data set, with the noise generator turned off. It therefore represents the highest SNR seen in this experiment.

The first reception shows a well-defined and rather obvious return at approximately 7.5m range from the source. The shape of this return clearly indicates the multi-path structure of the arrival. It can be seen visually that this return peaks at roughly 130mV.

When the signal is cut and time-reversed, as shown in the upper right graph, the structure of the return is even more apparent.

The lower right graph is the second reception. The return here is closer to 8m in range because that is the end point of the time-reverse window. The return is roughly 450mV peak amplitude, and sidelobes are well-defined and symmetric. Another noteworthy feature of the second reception is the noise level. Visually comparing the two
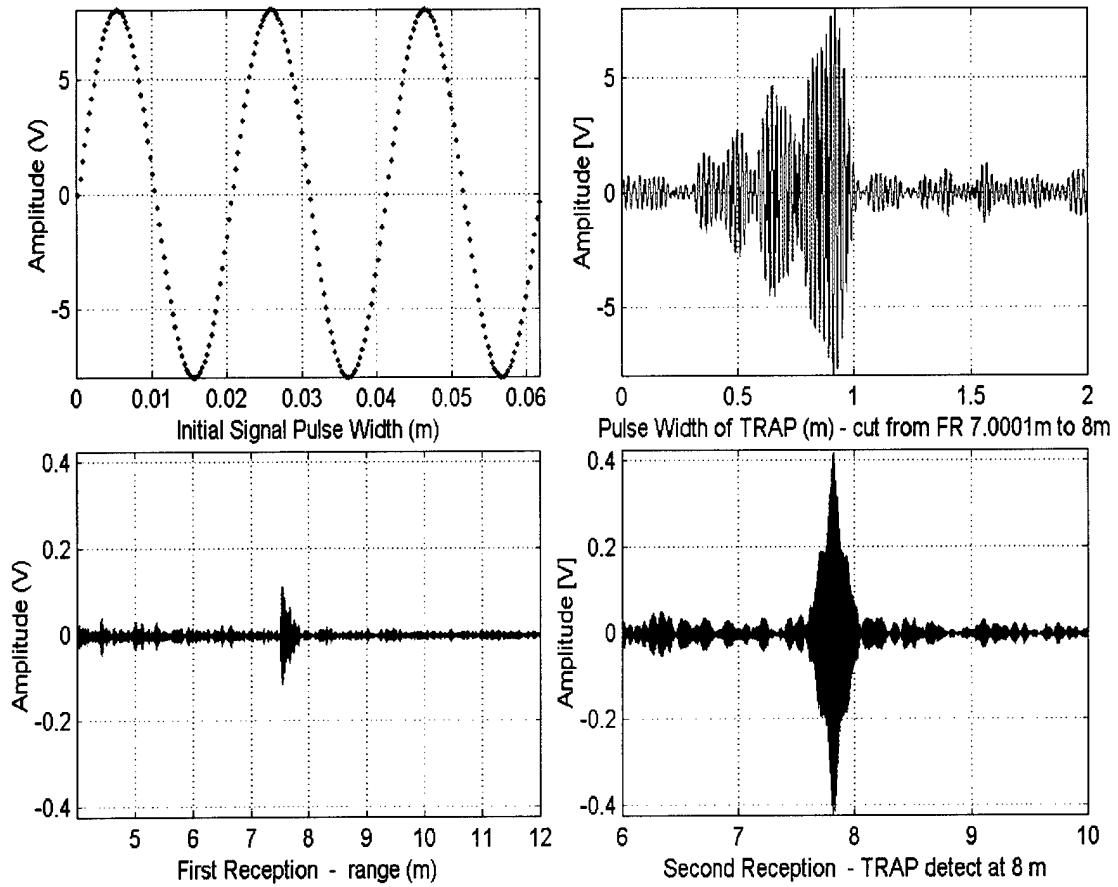
Figure 4.1   Sample TRAP data in the Low Noise Case, Recorded as T107n00.

graphs, the SR noise floor appears to be higher than the FR noise floor. This effect is due to the additional energy transmitted with the time-reversed signal.

It should be noticed that the peak of the SR return is not located at the target range. It is instead located at a point corresponding to the end of the capture range in the FR window. This detection in the SR window comes with a range ambiguity, then, on the order of the size of the TR window. This effect requires the target window for the SR calculations to be placed at 7.5-8.5m rather than the 7.0-8.0m in the first reception.

Examining Figure 4.1, however, one notes that the SR peak is not at 8.0m in range. The reason for this is a triggering delay in the oscilloscope cards. The first portion of the TR signal (approximately 40cm pulse width) does not exceed the trigger settings for the scope cards. This then causes a ~20cm shift in the SR peak range. At higher noise levels, the trigger level for the scope cards is reached almost instantly, and the SR peak is always at 8.0m.

When Equation 4.2 is applied to this sequence, resultant SNR is FR: +21.1dB, and +28.5dB in the SR. Each sequence in the N_00 data set was qualitatively similar to Figure 4.1. Further, as the noise generator was turned on and data were taken at its lowest output levels, the behavior of the TRAP sequences remained unchanged. The FR peak remained approximately 140mV, with evident modal structure visible in the FR and TR windows. The SR peak was always in excess of 400mV, and sidelobes were defined, but narrow. The pulse width of the SR return was approximately 50cm, including sidelobes. The pulse width of the narrow peak is roughly the same as the pulse width of the initial transmit signal. This is temporal focusing mentioned in Chapter I.

27

The sequences of the N_01 and N-02 data sets looked qualitatively like Figure 4.1, although the differences in the noise floor were visible.
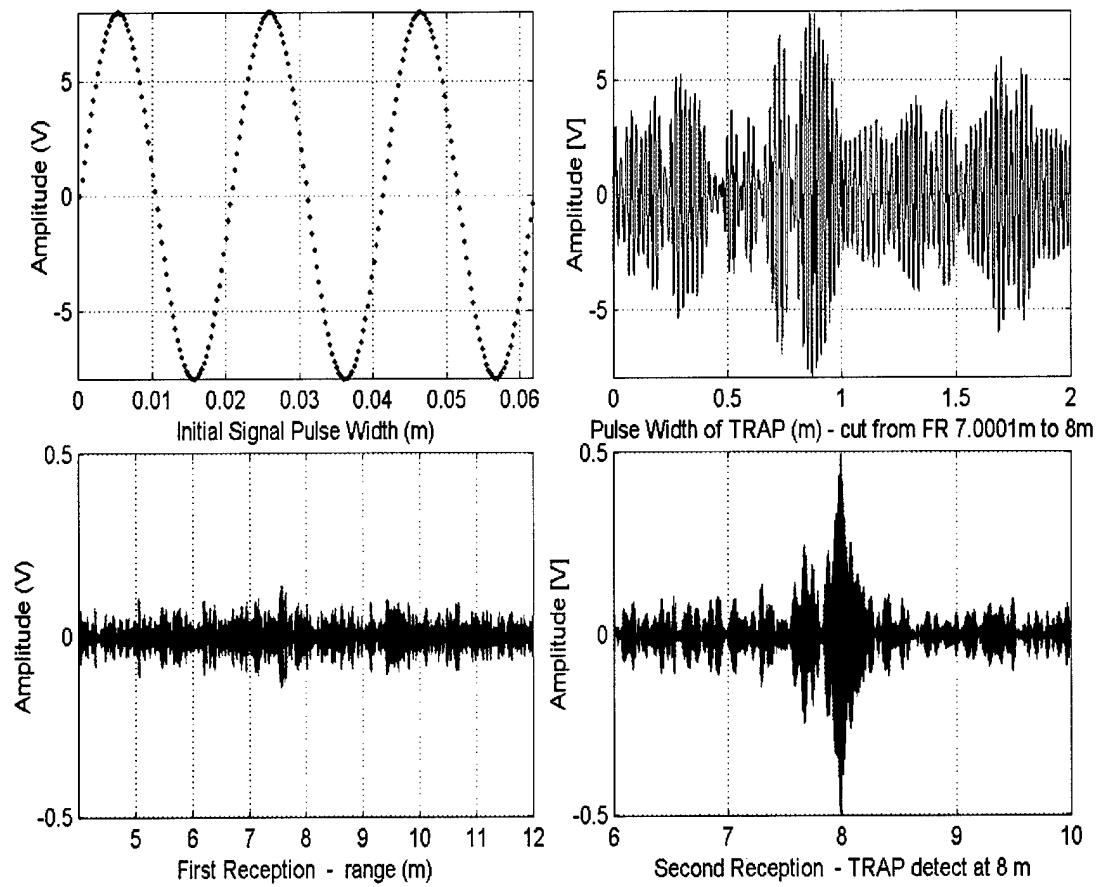
Figure 4.2   Sample TRAP data with moderate noise levels, Recorded as T127n04.

2. Moderate Noise

As noise level increased, the character of the first and second receptions began to change. Figure 4.2 shows a sample TRAP sequence from the N_04 data set.

In the example of Figure 4.2, the first reception shows a return at 7.5m that all but the alerted operator may have trouble distinguishing. SNR for this return is <+1dB, and there are a considerable number of noise spikes of magnitude comparable to the return. In other words, an operator selected detection threshold set low enough to detect the target return at 7.5m would also allow a number of false alarms, for example at 5.1m and 9.5m.

While this false alarm rate may still be considered acceptable, it is clear that the noise level in Figure 4.2 is approaching the limit for a reliable FR detection.

The TR signal plot can be seen as an expanded view of the first return. Notice that similar to the low noise situation, there is modal structure visible in this signal. This structure has a few features in common with the TR plot in Figure 4.1. It can be seen with equal clarity that there is a significant amount of non-signal being transmitted.

The second reception return in Figure 4.2 shows an SNR of +19dB. The character of this peak begins to change with increasing noise. The sidelobes tend to narrow, as does the central peak.

3. High Noise

Increasing the noise floor further will eventually mask the first reception. Figure 4.3 shows a sample TRAP sequence from the N_11 data set. In this example, even the alerted operator has no chance of distinguishing a target return at 7.5m. Even the TR window contains no discernable clue as to the existence of a target. Visual comparison between the TR windows in Figures 4.1 and 4.3 yield few similarities.

The second reception peak is still prominent. The symmetry of the sidelobes is diminished, but the magnitude of the peaks routinely exceeds 400mV. The calculated SNR from the sequence of Figure 4.3 is 0dB for the FR and +4.2dB for the SR.
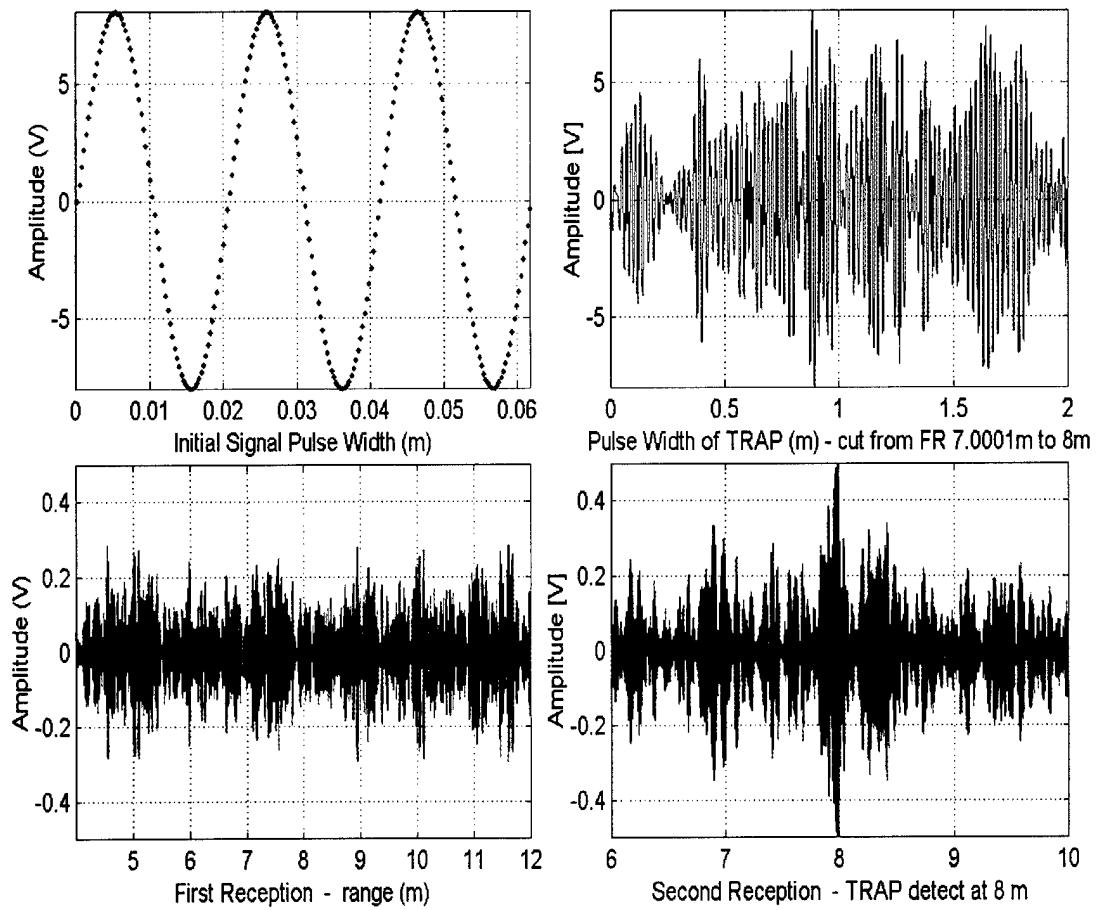
Figure 4.3   Sample TRAP sequence with high noise levels, Recorded as T115n11.

C. COMPARISON OF DATA SETS

When SNR has been calculated for the first and second reception for each TRAP sequence, it is possible to view them all on one graph, as shown in Figure 4.4. The horizontal scale of this graph is logarithmic, because SNR is a logarithmic quantity.

The first thing one notices is the overall trend of SNR v Noise for both the FR (in black) and the SR (in blue) is monotonically decreasing, with the same general slope. The separation of the curves suggested by the groups of data points represents the gain afforded by the time reversal process.

The lowest noise observed for the SR data is well above that of the FR. This is confirmation that the amount of "non-signal" transmitted with the time reversed information adds to the overall noise level.

The time reverse gain is not simply the vertical separation between the curves at a particular noise level. The added noise level must be considered. In Figure 4.4, the lowest data set N_00 can be clearly distinguished. The mean SNR for this data set is roughly 22dB for the FR and 29 dB for the SR. The gain is thus 7dB.

The increase in noise of the SR data due to transmission of non-signal is a smaller effect at higher noise levels. This is also seen in Figure 4.4, as the horizontal separation between the two groups of points tends to zero at the highest noise levels. . The mean gain in the higher data sets exceeds 10dB for this reason.

The overall mean in observed gain for this experiment was 7.3dB across all 714 TRAP sequences. The standard deviation in the observed gain was ±0.8dB.

Perhaps the largest advantage of the time reverse approach is the ability of this processing to produce a detectable return where there once was none. There were many TRAP sequences with a 0dB SNR in the FR that showed +3-5dB in the second reception. The presence of the SR peak at high noise levels (as in Figure 4.3) clearly demonstrates the system's ability to bring a target return out of the noise.
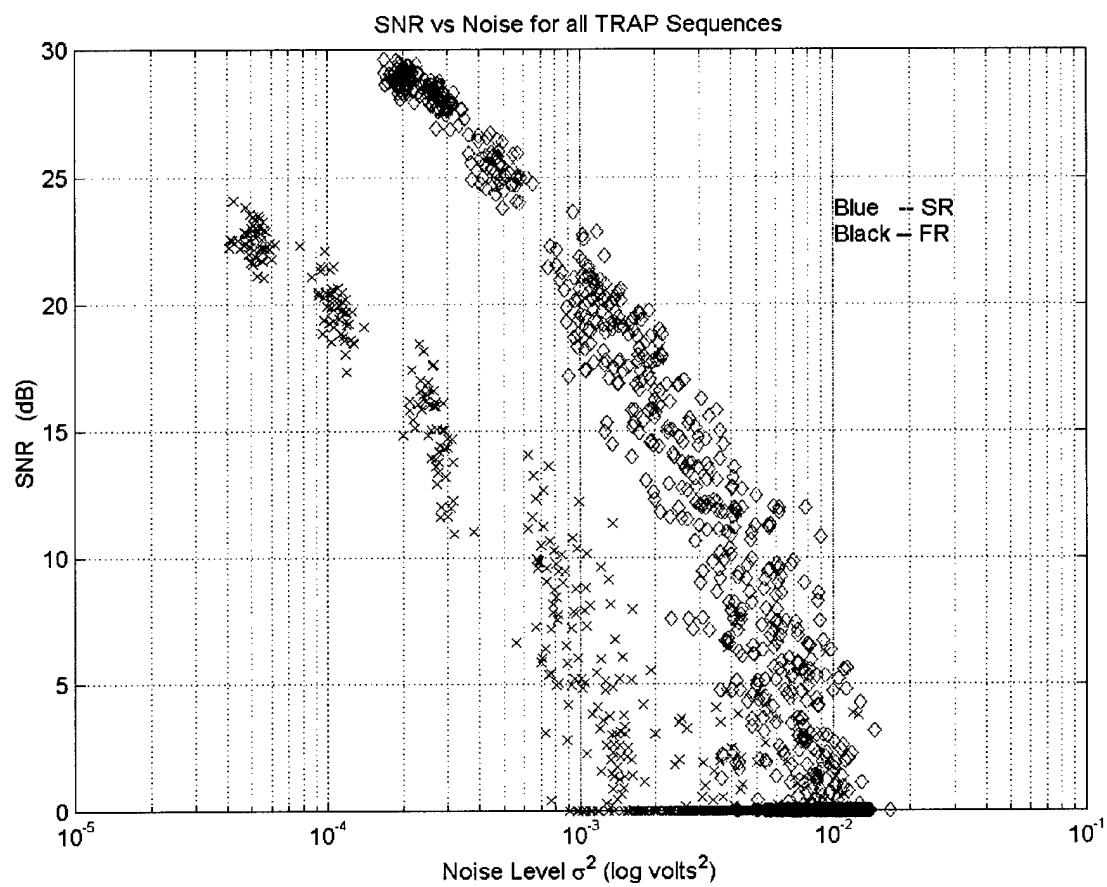
Figure 4.4   Scatter Plot Showing SNR Data From All TRAP Sequences.

These results do not significantly disagree with the expectations outlined in the theory of Chapter II. The 73kHz source in the Pekeris waveguide under test can be shown to excite no more than 5 modes that will be detectable in the range window 7.0-8.0m. Thus, the total number of sources in the virtual array created by applying the method of images to the two-way propagation is 10.

Khosla and Dowling (2001) stated that the expected time-reversal array gain in the presence of a noise field will be of the same order as the array gain of a vertical array of identical elements, i.e., $10\log_{10}(N)$ where N is the number of transducers in the time-reverse mirror. If the number of transducers in a virtual time-reverse mirror is assumed to be 10 (i.e., 2x5) then the expected array gain is:

$$10log_{10}(10) = 10\text{dB}. \tag{4.3}$$

Overall, the average time reverse gain is 7.3 ±0.8dB This is in reasonable agreement with the prediction of Equation 4.3. Note also that if the number of modes propagating were 4 instead of 5, then Equation 4.3 would yield an expected gain of 9dB.

V. CONCLUSIONS

A. SUMMARY OF RESULTS

These experiments have demonstrated that the time reversal process provides an enhanced detection for a single element sonar system. The test environment was a rather sterile ultrasonic laboratory waveguide, but the results obtained should translate to real ocean environments (Roux & Fink, 2000).

Overall, the average gain in reception SNR was 7.3 ±0.8dB over more than 700 individual TRAP sequences at varying noise levels. This value does not significantly disagree with the theoretical predictions for time-reverse array gain in a noisy environment as outlined by Khosla and Dowling (2001).

Used as an active sonar system, time-reverse acoustic processing shows promise for use in the littoral zones where the presence of in-band noise and multi-path propagation present so many limitations to current sonars. A possible employment scheme follows.

B. POSSIBLE EMPLOYMENT SCENARIO

As an example of the employment advantages such a system could offer, the following scenario is presented.

Consider a surface action group operating the relatively shallow water of the littorals. One of the serious threats to the security of this action group is the presence of slow-moving coastal patrol diesel submarines. The environment has a high ambient

noise level from many sources, including the heavy shipping traffic unrelated to military activities.

At some distance from the heart of the action group, a stationary surface ship is conducting a barrier search using a TRA-based active sonar. A separate TRAP sequence is transmitted at established time intervals, e.g., every five minutes. The time-reverse window establishes a constant annular region of intense scrutiny for the operators. When there is no target in the window, the time-reversed signal provides no return. At best, there is a stationary scatter source within the window that provides a constant, predictable return. When a target drives into the area, a new scatter source is present in the TR window, and a noticeable change in the second reception occurs.

The gain in reception level afforded by the TRAP sonar allows the operator to set the limits of the barrier to a longer range. That is, the nominal gain translates directly to detection range. This in turn translates to an increased reaction time before a potential adversary can approach to within weapons range. This further implies increased security for the surface action group.

C. RECOMMENDATIONS FOR FUTURE STUDY

Anything that would provide an active sonar system a nominal +11.7dB gain in a shallow ocean environment warrants further investigation. The success of applying TRA algorithms to single-element transmit/receive sonar in this experiment raises some interesting questions. These questions that must be scrutinized before any serious sea-going systems can be considered.

Nothing in this experiment (or in the body of references) is done which would intentionally interfere with the reciprocity of the waveguide. Time variations in the environment, noise field and target geometry are not considered. Kuperman et al, (1998) performed ocean experiments using time-reversal in which he was able to demonstrate that a time-reversed pulse produced a retrofocus up to a week after the initial transmission. The variations in the environment in those cases were minor, but overall, the robustness of the process seems promising. It would be interesting to quantify the changes in the SR peak resulting from controlled changes to the water column. A time-varying thermal gradient and introduction of body waves or currents are two examples. A field of bubbles might also be used to yield quasi-static noise and scatter sources.

In applications of TRA involving time reversal mirrors with a large number of elements, the process of iterative time reversal has been explored to tighten the focus of acoustic energy, and to discriminate among targets. There are algorithms, for instance, which make it possible to enhance either the weaker or the stronger of two nearby returns. Experiments should therefore be run with targets of different strength to see if the single element time-reversal process in the waveguide can produce enough resolution to selectively focus on weaker/stronger targets.

THIS PAGE INTENTIONALLY LEFT BLANK

LIST OF REFERENCES

Fink, M. (1997), "Time Reversed Acoustics", Physics Today, March 1997, pp.34-40

Fink, M (1998), "Ultrasound Puts Materials to the Test", NDTnet, 1998 April, Vol. 3 No. 4

Heinemann, G., *Experimental Studies of Applications of Time-Reversal Acoustics to Non-Coherent Underwater Communications*, Master's Thesis, Naval Postgraduate School, Monterey, California, March 2000

Jensen, F.B., Kuperman, W.A., Porter, M.B., Schmidt, H., "Computational Ocean Acoustics", *American Institute of Physics*, 2000

Khosla, S.R., Dowling, D.R., (2001) "Time Reversing Array Retrofocusing in Noisy Environments", *Journal of the Acoustical Society of America* Vol. 109 pt. 2, pp.-538-546

Kinsler, L.E., Frey, A.R., Coppens, A.B., Sanders, J.V., *Fundamentals of Acoustics*, 4th ed, John Wiley & Sons, 2000

Kuperman, W.A., Hodgkiss W.S., Song, H.C., Akal, T., Ferla, C., Jackson, D.R., (1998), "Phase Conjugation in the Ocean: Experimental Demonstration of an Acoustic Time-Reverse Mirror", *Journal of the Acoustical Society of America*, Vol. 103, pt. 1, pp. 25-40

Parvulescu, A., (1995) "Matched Signal (MESS) Processing by the Ocean", *Journal of the Acoustical Society of America*, Vol. 98. pp. 943-960

Roux, P., Fink, M. (2000) "Time Reversal in a Waveguide: Study of the Temporal and Spatial Focusing", *Journal of the Acoustical Society of America*, Vol. 107, No. 5, pt. 1, pp. 2418-2429

THIS PAGE INTENTIONALLY LEFT BLANK

INITIAL DISTRIBUTION LIST

1. Defense Technical Information Center 2
   8725 John J. Kingman Road, Suite 0944
   Ft. Belvoir, VA 22060-6218

2. Dudley Knox Library 2
   Naval Postgraduate School
   411 Dyer Road
   Monterey, CA 93943-5101

3. Engineering and Technology Curricular Office (Code 34) 1
   Naval Postgraduate School
   700 Dyer Road, Room 115
   Monterey, CA 93943-5107

4. Mitchell N. Shipley 2
   203 Applied Science Building
   Applied Research Lab
   Penn State University
   P.O. Box 30
   State College, PA 16804-0030

5. Prof. A Larraza, Code PH/La 4
   Department of Physics
   Naval Postgraduate School
   Monterey CA 93943-5002

6. Prof. W. Maier, Code PH/Mw 2
   Department of Physics
   Naval Postgraduate School
   Monterey, CA 93943-5002

7. Mr William Glenney 1
   Deputy Director
   CNO Strategic Studies Group
   686 Cushing Road
   Newport, RI 02841-1207

8. LCDR John P. Stokely 1
   2911 Folklore Drive
   Tampa, FL 33594